Silver nanoparticles, ions, and shape governing soil microbial functional diversity: Nano Shapes Micro

Zhai, Y.; Hunting, E.R.; Wouters, M.; Peijnenburg, W.J.G.M.; Vijver, M.G.

frontiers in Microbiology

ORIGINAL RESEARCH
published: 25 July 2016
doi: 10.3389/fmicb.2016.01123

Silver Nanoparticles, Ions, and Shape Governing Soil Microbial Functional Diversity: Nano Shapes Micro

Yujia Zhai[1], Ellard R. Hunting[1], Marja Wouters[2], Willie J. G. M. Peijnenburg[1,2] and Martina G. Vijver[1]*

[1] Institute of Environmental Sciences, Leiden University, Leiden, Netherlands, [2] National Institute of Public Health and the Environment, Bilthoven, Netherlands

Silver nanoparticles (AgNPs) affect microbial metabolic processes at single cell level or lab-culture strains. However, the impact of different AgNPs properties such as the particle, ion release, and shape on functional responses of natural soil microbial communities remain poorly understood. Therefore, we assessed the relative importance of particles and ions of AgNPs in bacterial toxicity and how the functional diversity of soil microbial communities were impacted by AgNPs shapes (i.e., plates, spheres, and rods) in laboratory incubations. Our results showed that the relative contribution of $AgNPs_{(particle)}$ increased with increasing exposure concentrations (accounted for about 60–68% of the total toxicity at the highest exposure level). In addition, the functional composition of the microbial community differed significantly according to different AgNPs shapes. The various properties of AgNPs thus can significantly and differentially affect the functional composition of microbial communities and associated ecosystem processes depending on the level of environmental exposure.

Keywords: nanosilver, Biolog Ecoplates, nanoecotoxicology, microbial community, functional diversity

OPEN ACCESS

Edited by:
Prayad Pokethitiyook, Mahidol University, Thailand

Reviewed by:
Sung-Woo Lee, Oregon Health & Science University, USA
Jay Prakash Verma, Banaras Hindu University, India

****Correspondence:***
Yujia Zhai
y.zhai@cml.leidenunv.nl

Specialty section:
This article was submitted to Microbiotechnology, Ecotoxicology and Bioremediation, a section of the journal Frontiers in Microbiology

Received: *17 May 2016*
Accepted: *06 July 2016*
Published: *25 July 2016*

Citation:
Zhai Y, Hunting ER, Wouters M, Peijnenburg WJGM and Vijver MG (2016) Silver Nanoparticles, Ions, and Shape Governing Soil Microbial Functional Diversity: Nano Shapes Micro. Front. Microbiol. 7:1123. doi: 10.3389/fmicb.2016.01123

INTRODUCTION

Silver nanoparticles (AgNPs) are known for their anti-microbial properties and are broadly used in clothing, food industry, cosmetics, and medical devices (Kendra and Arturo, 2014; Theophel et al., 2014). Likely resulting from these industrial and medical applications, AgNPs are reported to end up in both soils and aquatic sediments (e.g., Schlich et al., 2013; Yu et al., 2013; McKee and Filser, 2016), with inherent risks for natural microbial communities that play a pivotal role in the functioning of ecosystems (Lau and Lennon, 2012).

While most studies have focused on AgNPs toxicity on single bacterial species under laboratory conditions (e.g., Pal et al., 2007; McQuillan et al., 2011; Levard et al., 2012), a number of studies also provided evidence that small size metal NPs are detrimental to natural soil microbial communities (Dinesh et al., 2012), affecting community composition (Kumar et al., 2011; Echavarri-Bravo et al., 2015; Sillen et al., 2015), bacterial biomass (Hänsch and Emmerling, 2010), and bacterial processes (Ge et al., 2011). Toxicity of AgNPs suspensions, however, can be ascribed to the properties of the nanoparticles and/or to dissolved ions released from the AgNPs. Which property dominates toxicity appears contradictive as exposure of various bacterial and fungal species to both particle species and ion species of AgNPs has to date revealed that both species can be very important (cf. Levard et al., 2013; González et al., 2015; Tlili et al., 2016). Moreover, most studies evaluating the relative importance of particle species and ion species of AgNPs were restricted to single bacterial species/strains, and therefore, the relative contributions of particle species and ion species of AgNPs to natural microbial communities remain uncertain.

In addition to ion and particle effects, the particle attributes size and in particular shape have been well documented to determine toxicity of NPs in laboratory cultures. Ivask et al. (2014) analyzed the toxicity of different sized AgNPs on a variety of species showed that responses were often size-dependent, having the highest impact with small particles. Additionally, the shape showed to have an impact on responses, e.g., George et al. (2012) reported that silver nanoplates were considerably more toxic than spheres and wires. Moreover, silver nanocubes displayed a lower toxicity compared to quasi-spherical silver nanoparticles and silver nanowires (Gorka et al., 2015). However, a comprehensive understanding on the effect of AgNPs shape on natural microbial communities is currently lacking. Therefore, whether AgNPs shape governs microbial functional diversity on the community level requires investigation.

The present study aims to evaluate: (i) the relative contribution of particle species and ion species of AgNPs to the overall toxicity on microbial carbon substrate utilization as a relevant functional endpoint and (ii) the impact of AgNPs shape on the functional diversity of soil microbial communities. To this end, natural soil microbial communities were exposed to different concentrations and shapes (spheres, plates, and rods) of AgNPs in laboratory incubations.

MATERIALS AND METHODS

Nanoparticles and Reagents

AgNP 50–80 nm nanoplates (stored as 450 mg/L Ag dispersions in polyvinylpyrrolidone) were obtained from Moscow State University (Moscow, Russia). A dispersion of AgNP 15 nm nanospheres [particle size 15 nm, 10.16% Ag (w/w) in a stabilizing vehicle material consisting of polyoxyethylene glycerol trioleate (4%; w/w) and polyoxyethylene (20) sorbitan monolaurate (Tween 20; 4%; w/w; manufacturer's information) (Van der Ploeg et al., 2014)] was obtained from a commercial source (Nanostructured & Amorphous Materials, Houston, TX, USA); AgNP 20–40 nm nanospheres (particle size range 20–40 nm, powder) were manufactured by a patented vapor condensation process from QSI-Nano® (Santa Ana, CA, USA); AgNP 50 nm nanorods (with reported width of 50 nm and length of 5–10 μm, dispersion of 8.6% Ag (w/w) in an aqueous solution containing polyvinylpyrrolidone (<1% w/w), acrylic/acrylate copolymer (<2% w/w) and polycarboxylate ether (<2% w/w)) (Hund-Rinke and Schlich, 2014) were supplied by the Fraunhofer Institute (Schmallenberg, Germany). $AgNO_3$ was purchased from Sigma–Aldrich (Zwijndrecht, Netherlands).

Physio-chemical characterizations of AgNPs were done following the risk assessment of engineered nanoparticles (ENPRA) nanomaterial dispersion protocol for toxicological studies (Kermanizadeh et al., 2012). The stock suspension was sonicated for 8 min (in 4°C water, twice) at 38 ± 10 KHz, and diluted in BIS–TRIS buffer. During this dilution process the primary AgNPs dispersions were continuously inverted and vortexed to prevent the particles from sedimentation. Characterization of particle size and morphology of the four kinds of AgNPs were analyzed using transmission electron microscopy (TEM; JEOL 1010, IEOL Ltd., Japan). Size distribution of AgNPs suspensions were analyzed at 1, 24, and 96 h after incubation in the exposure medium by dynamic light scattering (DLS, Malvern, Instruments Ltd., UK). Concentrations of AgNPs suspensions (designated as $AgNPs_{(total)}$ hereafter) in the exposure media were determined using Atomic Absorption Spectroscopy (AAS; Perkin Elmer 1100B) at 1, 24, 48, 72, and 96 h. The Ag-ion concentrations released from the $AgNPs_{(total)}$ at 1 mg/L in test media were also measured at the same times.

Natural Soils and Microbial Community

Soil samples were collected from a site dominated by deciduous trees (52°07'06.7″N 5°11′23.1″E, Bilthoven, Netherlands). Moist soil samples were selected and sieved with an 8-mm sieve and kept at 4°C for the duration of the experiments. The soil moisture content was maintained at the initial content which was 18.4% of the dry soil weight by regularly supplying distilled water. Subsequently, 60 g soil subsamples were placed in glass jars and incubated for 120 h. Ten grams of this soil sample was added to 90 mL of 10 mM (2.09 g/L) BIS–TRIS (Sigma–Aldrich B9754). This buffer was adjusted to pH 7 using 1 M HNO_3. The buffer with soil added was then centrifuged for 10 min at 1500 rpm, after which the supernatant was filtered (to remove the soil particles) and diluted five times with the same buffer (soil microbial community extract).

Experimental Outline

A 15 mL soil extract of 1% w/v soil microbial community extract was added to the different silver suspensions treatments. Exposure concentrations were selected to range from 0.070 to 0.678 mg/L for the 50–80 nm nanoplates, 0.072 to 0.708 mg/L for the 15 nm nanospheres, from 0.108 to 0.814 mg/L for the 20–40 nm nanospheres and from 0.141 to 1.529 mg/L for the 50 nm nanorods based on range finding experiments. The effect of $AgNO_3$ was tested in the range from 0.003 to 0.05 mg/L as a positive reference to assess the toxicity of Ag^+. Considering the rapid aggregation process of nanoparticles, the soil microbial community extracts were exposed to AgNPs for less than 2 h. To obtain a solution of the ion species of AgNPs, the AgNPs suspensions were centrifuged at 30,392*g* for 30 min (Sorvall RC5Bplus centrifuge, Fiber lite F21-8 × 50 year rotor) and filtered by a filter with 0.02 μm pore diameter. This step yields supernatants with negligible amounts of particles (Hua et al., 2014), which were used as Ag-ion suspension. $AgNP_{(ion)}$ was operationally defined as the Ag measured in the supernatant. Accordingly, $AgNP_{(particle)}$ is the difference between the Ag measured in the AgNP suspension and $AgNP_{(ion)}$.

Community metabolic diversity was determined by evaluating the carbon substrate utilization patterns using commercial Ecoplates (Biolog, Hayward, CA, USA; Garland and Mills, 1991) containing 3 times 31 carbon sources (Supplementary Table S1). Biolog Ecoplates are comprised of ecologically relevant, structurally diverse compounds, yet do not include e.g., recalcitrant substrates nor specific substrates typical of the soils used in this study. It is therefore impossible to directly relate substrate utilization profiles to the actual functioning of the soil microbial communities. Nonetheless, the number

of substrates used can serve as a proxy of the metabolic diversity of the microbial community (Garland, 1999; Krause et al., 2014). Moreover, differences in utilization profiles indicate that functionally distinct microbial communities can develop depending on treatment (e.g., Hunting et al., 2013a,b, 2015; Wang et al., 2015). Each well of the Biolog Ecoplates was inoculated with 100 μl of supernatant extracted from different AgNPs exposed soil samples as described above, and incubated for 96 h at 20°C, to enhance microbial growth. Optical density (OD) was measured at 590 nm (OD_{590}) immediately after inoculation of the plates and at 24, 48, 72, and 96 h to ensure that a saturation of the utilization rate in all samples was reached.

Data Analysis

The average OD_{590} of each carbon source (three replicates) was calculated for each measurement. Average well color development (AWCD) was used to represent the average microbial metabolic activity. AWCD was calculated for the 31 substrates as described by (Garland and Mills, 1991) and transformed (Weber et al., 2007).

The transformed values of AWCD of soil extracts exposed to AgNPs were used as the total effect ($E_{(total)}$). The effect of $AgNO_3$ was also tested in order to allow to calculate the effect of ions released from the corresponding AgNPs ($E_{(ion)}$). The response addition model (RA) was used to calculate the relative contribution to toxicity of $AgNPs_{(particle)}$ and $AgNPs_{(ion)}$ because different mechanistic pathways of $NP_{(particle)}$ and $NP_{(ion)}$ were assumed, according the assumptions of Hua et al. (2014):

$$E_{(\text{total})} = \left(\left(1 - E_{(\text{ion})}\right)\left(1 - E_{(\text{particle})}\right)\right)$$

Substrate utilization was chosen as the transformed OD_{590} value greater than 0.25. Shannon indices (Shannon, 1948) were also calculated for each microbial community exposed to differently AgNPs as a measure of the diversity of the microbial communities active during incubation.

The exposure concentrations for each AgNPs are subject to exponential decay as they decrease along with time. This dissociation model heads downhill gradually reaching a plateau (P). The dynamics of the exposure concentrations were accounted using the time weighted average (TWA) concentrations for $AgNPs_{(total)}$ and $AgNPs_{(particle)}$ (1–96 h) depending on the nonlinear fit of ion release profiles:

$$C = (C_0 - P) \ * \ e^{(-K * T)} + P$$

where C_0 is the C (concentration, mg/L) value when T (time, h) is zero. P is the C value at infinite times. K is the rate constant. Statistics of the nonlinear fit of ion release profiles for each $AgNPs_{(total)}$ and $AgNPs_{(particle)}$ are shown in Supplementary Table S2.

The EC_x values were based on TWA concentrations for $AgNPs_{(total)}$ and $AgNPs_{(particle)}$ and calculated by the dose–response-inhibition model in GraphPad Prism 6.0. Statistically significant differences between different soil extracts exposed to four AgNPs were determined by a two-way ANOVA and Turkey's honestly significant difference tests (with significance level set as $p < 0.05$). To relate the microbial functional composition under four AgNPs exposure levels, the 31 carbon substrates utilization were analyzed using a Euclidean-based cluster analysis and a two-way analysis of similarities (ANOSIM) in PAST 3.0. (Hammer et al., 2001; Villéger et al., 2008).

RESULTS

Physicochemical Characterization of AgNPs

Transmission electron microscopy images reflecting the different shapes and primary sizes of the four AgNPs are shown in Supplementary Figure S1. Data on size distributions after 1, 24, 48, and 96 h are given in **Table 1**. It can be seen that AgNPs aggregated directly after submerging into the exposure medium. The particle sizes in the exposure medium changed from 191, 196, 187, and 288 nm after 1 h of incubation to 368, 385, 373, and 496 nm after 96 h of incubation, respectively. The 96 h ion release profiles of AgNPs are shown in **Figure 1**. It can be seen that the percentage of $AgNP_{(ion)}$ in the AgNPs suspension at 1 mg shifted from 10, 8, 12, and 4% after 1 h to 13, 10, 14, and 6% after 96 h of incubation in the buffer, respectively.

The 96 h Toxicity of AgNPs and $AgNO_3$

The dose–response curves of $AgNPs_{(total)}$ and $AgNO_3$ based on the TWA concentrations are provided in **Figure 2A**. As described above, toxicity was expressed as the values of AWCD. It can be seen that all exposures of the microbial community to the nanoparticle suspensions induced significant toxicity. The 50–80 nm $nanoplates_{(total)}$, 15 nm $nanospheres_{(total)}$ and 20–40 nm $nanospheres_{(total)}$ showed much lower 96 h EC_{50} values compared to that of 50 nm $nanorods_{(total)}$. The EC_{50} value derived from the $AgNO_3$ curve was 0.064 mg/L, which implied that the Ag^+ was the most toxic among all the different silver species tested.

The dose–response curves of $AgNPs_{(particle)}$ based on the TWA concentrations are provided in **Figure 2B**. These curves could be derived after using the RA model. The 50–80 nm $nanoplates_{(particle)}$, 15 nm $nanospheres_{(particle)}$ and 20–40 nm $nanospheres_{(particle)}$ showed much lower 96 h EC_{50} values of 0.201 mg/L, 0.212 mg/L and 0.222 mg/L, respectively, compared to the 50 nm $nanorods_{(particle)}$ (0.342 mg/L), which indicated that

TABLE 1 | Hydrodynamic diameter of 1 mg/L suspensions of silver nanoparticles (AgNPs) in the exposure medium.

	Hydrodynamic diameter (nm)[a]			
Type	**1 h**	**24 h**	**48 h**	**96 h**
50–80 nm nanoplates	196 ± 15	352 ± 27	368 ± 41	382 ± 54
15 nm nanospheres	191 ± 12	346 ± 42	385 ± 36	393 ± 78*
20–40 nm nanospheres	187 ± 5	337 ± 13	373 ± 21	387 ± 76*
50 nm nanorods	288 ± 20	463 ± 48	487 ± 76	496 ± 148*

[a]*Hydrodynamic diameter are expressed as mean ± SD (n = 3). *Statistical analysis was used to compare the significant difference of hydrodynamic diameter between 1 and 96 h ($p < 0.05$).*

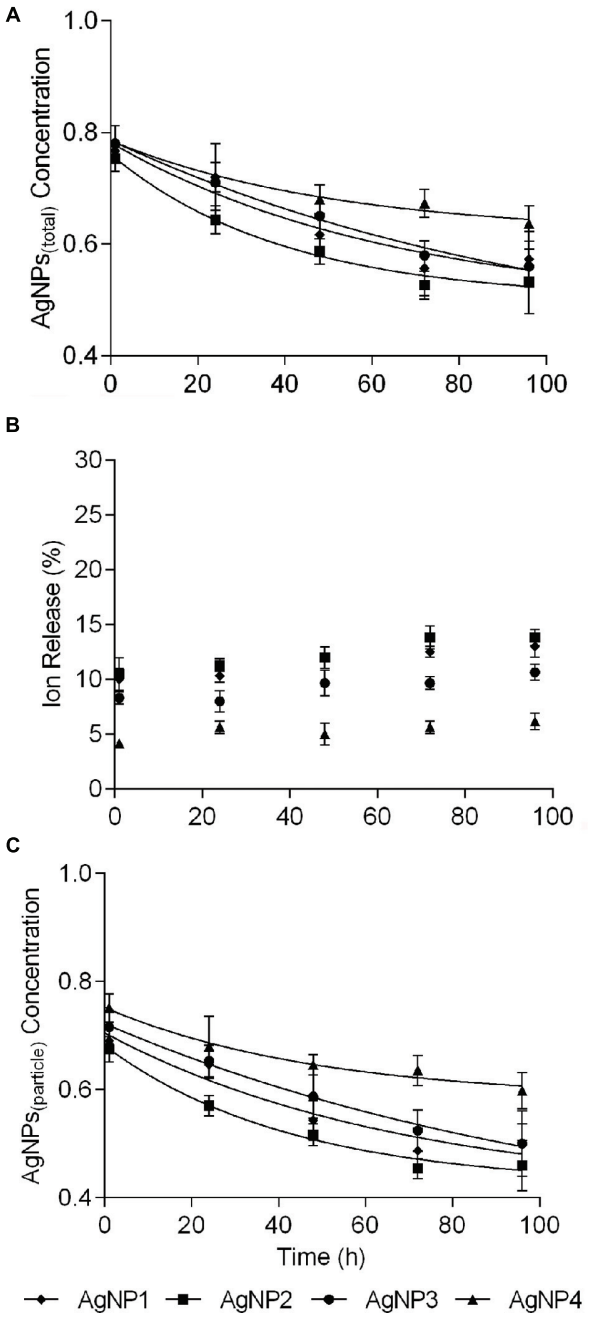

FIGURE 1 | Ion release profiles of silver nanoparticles (AgNPs) at 1 mg/L, during 96 h of incubation in the exposure medium. (A) Total Ag concentrations of the $AgNPs_{(total)}$. **(B)** Relative percentage of dissolved Ag released from AgNPs. **(C)** Ag concentrations of the $AgNPs_{(particle)}$. Data are mean ± SD ($n = 3$). (AgNP1:50–80 nm nanoplates, AgNP2:15 nm nanospheres, AgNP3:20–40 nm nanospheres, and AgNP4:50 nm nanorods).

the 50–80 nm nanoplates, 15 nm nanospheres and 20–40 nm nanospheres were much more toxic to soil microbes, compared to the 50 nm nanorods.

The dose–response curves based on initial concentrations of the differently sized and shaped AgNPs on the catabolic capabilities of a microbial community are shown in Supplementary Figure S3. The EC_{50} values of $AgNPs_{(total)}$ and $AgNPs_{(particle)}$ using TWA versus initial concentrations are summarized in **Table 2**.

Relative Contribution to Toxicity of $AgNPs_{(particle)}$ and $AgNPs_{(ion)}$

The relative contributions of $AgNPs_{(particle)}$ and $AgNPs_{(ion)}$ to the overall toxicity of AgNPs to a microbial community at different effect levels is given in **Table 3**. At the EC_{20} level, the contributions of 50–80 nm $nanoplates_{(particle)}$, 15 nm $nanospheres_{(particle)}$, 20–40 nm $nanospheres_{(particle)}$, and 50 nm $nanorods_{(particle)}$ to the overall toxicity were 32–43%. The contribution to toxicity of the particles increased with increasing exposure concentrations. The 50–80 nm $nanoplates_{(particle)}$, 15 nm $nanospheres_{(particle)}$, 20–40 nm $nanospheres_{(particle)}$, and 50 nm $nanorods_{(particle)}$ accounted for about 60–68% of the relative contribution to toxicity at the EC_{90} level of the suspensions.

Community Metabolic Diversity

Toxic effects of AgNPs to the soil microbial community were mainly reflected in a change of the community metabolic diversity. Thus, the functional diversity of microbial communities under the four different AgNPs treatments needed to be further explored. **Figure 3** presents the Shannon index of microbial communities under the four different AgNPs treatments at the EC_{20}, EC_{60}, and EC_{90} levels. The values of Shannon index decreased with increasing exposure concentrations. No significant difference was observed between the 20–40 nm and 15 nm nanospheres exposure. In contrast, 50–80 nm nanoplates and 50 nm nanorods exposure significantly reduced the community metabolic diversity ($p < 0.05$).

Patterns in carbon substrate utilization reflected differences in the functional diversity of the microbial communities among different AgNPs treatments (Supplementary Figure S2 and **Figure 4**). The microbial communities in the control soil extracts were in general able to metabolize 20 of the 31 carbon sources, and the utilization of most of the substrates decreased with the increasing AgNPs concentrations (Supplementary Figure S2). At the EC_{20} level, the utilization of Glycogen was inhibited in all AgNPs exposed microbial communities, however, the ability of microbial communities to utilize Glycyl-L-glutamic acid was stimulated by the AgNPs exposure. At the EC_{60} level, the similar pattern of carbon utilization was only obtained in microbial communities under treatment of 15 and 20–40 nm nanoshperes, which suggested that microbial efficiency in exposure of spherical AgNPs was similar. At the EC_{90} level, exposure to AgNPs significantly inhibited utilization of all substrates ($p < 0.05$).

Figure 4 shows the cluster analysis of the carbon source metabolisms of the microbial communities under the four AgNPs treatments at the EC_{20}, EC_{60}, and EC_{90} levels. Microbial metabolic diversity differed significantly between treatments depending on both EC levels and shapes (two-way ANOSIM: EC level $R = 0.953$, $p < 0.05$; shape $R = 0.876$, $p < 0.05$), showing that the developed microbial communities were functionally distinct.

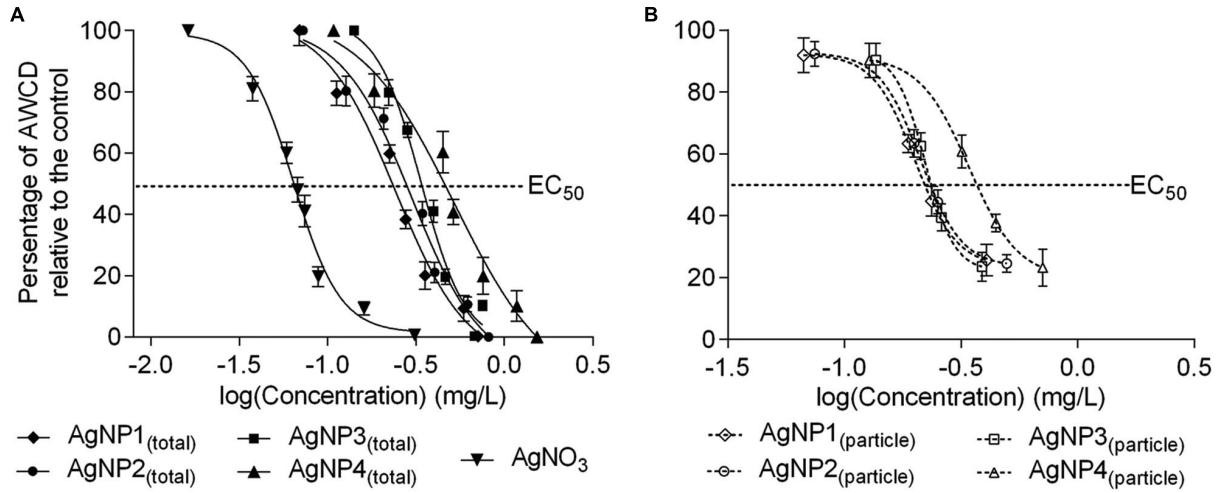

FIGURE 2 | Dose–response curves of average well color development (AWCD) of soil extracts exposed to suspensions of (A) $AgNPs_{(total)}$ and $AgNO_3$, and (B) $AgNPs_{(particle)}$ expressed as time weighted concentrations. AWCD are plotted on the *y*-axis, actual log-transformed Ag concentrations are plotted on the *x*-axis. Data are mean ± SD ($n = 3$). (AgNP1:50–80 nm nanoplates, AgNP2:15 nm nanospheres, AgNP3:20–40 nm nanospheres, and AgNP4:50 nm nanorods).

DISCUSSION

In this study, we found that the dissolution of AgNPs at 1 mg/L increased with time, with 6–13% of the Ag-ion released after 96 h of incubation (**Figure 1**). This was similar to the result obtained by Zhao and Wang (2012) who detected that less than 10% of Ag release from AgNPs at an initial concentration of 1 mg/L. The ion release profiles of NPs was a combined effects affected by the physio-chemical characteristics of NPs, such as particle size, shapes, initial concentrations of NPs and so on

TABLE 2 | The EC_{50} values of $AgNPs_{(total)}$ and $AgNPs_{(particle)}$ expressed on initial concentrations and expressed on time weighted average concentrations.

		EC_{50} (mg/L)[a]		95% Confidence intervals	
		Total	Particle	Total	Particle
Initial concentrations	50–80 nm nanoplates	0.354	0.228	0.331–0.506	0.216–0.242
	15 nm nanospheres	0.409	0.249	0.318–0.394	0.227–0.267
	20–40 nm nanospheres	0.535	0.313	0.487–0.715	0.234–0.264
	50 nm nanorods	0.590	0.402	0.376–0.763	0.361–0.446
TWA[b]	50–80 nm nanoplates	0.242	0.201	0.205–0.286	0.184–0.220
	15 nm nanospheres	0.299	0.212	0.255–0.351	0.198–0.227
	20–40 nm nanospheres	0.337	0.222	0.307–0.369	0.207–0.237
	50 nm nanorods	0.521	0.342	0.380–0.714	0.302–0.387

[a]*EC_{50} is half maximal effective concentration.* [b]*TWA is time weighted average concentration.*

TABLE 3 | Relative contribution of particles and shedding ions of AgNPs to toxicity at different effect levels of nanoparticle suspensions.

		50–80 nm nanoplates		15 nm nanospheres		20–40 nm nanospheres		50 nm nanorods	
		Conc. (mg/L)	Contrib. (%)	Conc. (mg/L)	Contrib. (%)	Conc. (mg/L)	Contrib. (%)	Conc. (mg/L)	Contrib. (%)
EC_{20}	Particle	0.067	32	0.075	33	0.137	40	0.176	43
	Ion	0.045	68	0.052	67	0.085	60	0.092	57
EC_{60}	Particle	0.188	53	0.199	55	0.213	58	0.383	62
	Ion	0.087	47	0.144	45	0.184	42	0.194	38
EC_{80}	Particle	0.237	58	0.251	61	0.260	62	0.447	68
	Ion	0.118	42	0.152	39	0.203	38	0.310	32
EC_{90}	Particle	0.307	60	0.327	63	0.389	64	0.708	68
	Ion	0.182	40	0.193	37	0.209	36	0.467	32

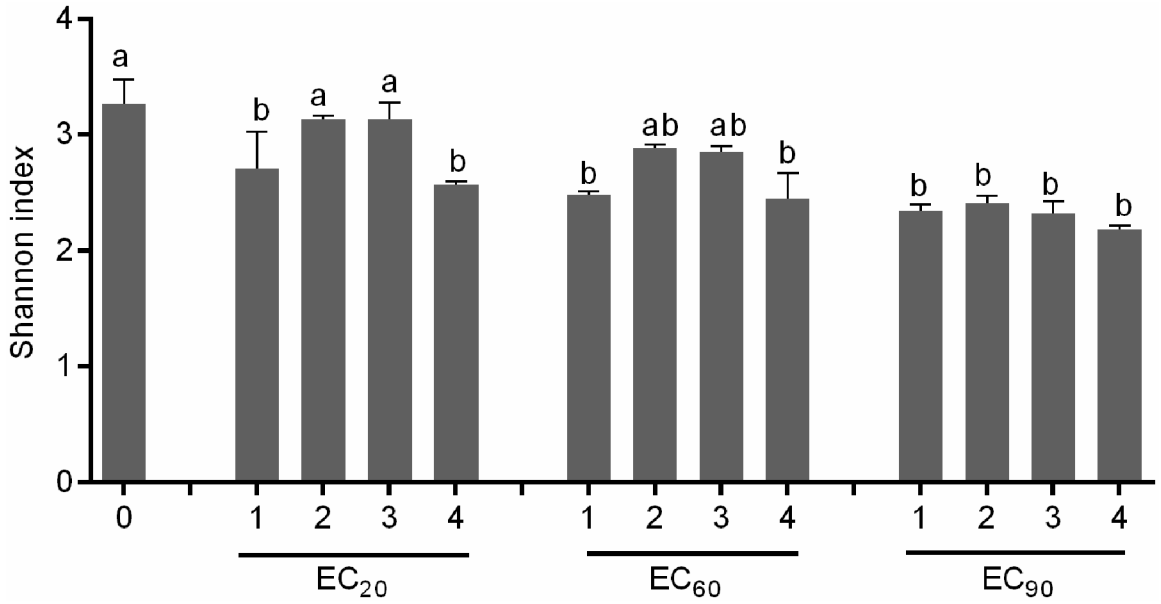

FIGURE 3 | Functional diversity of microbial communities under the four different AgNPs treatment at the EC_{20}, EC_{60}, and EC_{90} levels. The bars are the standard errors of the means ($n = 3$). The different letters above the bar in the same EC level indicate significant differences between different treatments at $p < 0.05$ level (0-control, 1:50–80 nm nanoplates, 2:15 nm nanospheres, 3:20–40 nm nanospheres, and 4:50 nm nanorods).

(Yang et al., 2014). In our case, the nanoplates AgNPs were demonstrated to be more soluble than the other shapes of AgNPs in the exposure media, and the ion release of nanorods AgNPs were the lowest. Expressing the exposure concentration based on TWA accounts for declining trends in the exposure over time and variability between NP species, and hence gave a more accurate display for exposure concentrations as experienced by microorganisms compared to expressing responses based on the initial concentrations. This decline in exposure concentration also made that the EC_{50} values lower based on TWA than on the initial concentration, and the EC_{50} values of $AgNPs_{(particle)}$ got lumped together for the 50–80 nm nanoplates, 15 nm nanospheres, 20–40 nm nanospheres, and even 50 nm nanorods came more close. Currently, we cannot explain this phenomenon, but it does mean that the toxicity irrespective of the shape is more or less similar, and that the difference within the overall response (expressed as EC_{50} values for $AgNPs_{(total)}$) more likely can be explained by differences in ion shedding from the different shaped particles. Since initial concentrations is currently the most widely used way of expressing the fate of nanoparticles in exposure medium, we incorporated this as well to allow comparison with earlier reported studies. However, based on our observations, we strongly encourage to use TWA concentrations as the TWA approach can capture the condition-related dynamic changes of NPs in exposure medium.

The relative contributions of ions and particles in the effect of NPs on natural microbial communities to date remain uncertain. Previous studies have focused more on the toxicity of AgNPs suspensions. Topuz and van Gestel (2015) concluded that the toxicity of citrate-coated AgNPs and polyvinylpyrrolidone-coated AgNPs on *Enchytraeus crypticus* probably was mainly attributable to $AgNPs_{(ion)}$. Our results showed that at lower exposure concentrations (EC_{20} level), the contribution of the $AgNPs_{(ion)}$ was higher than those of $AgNPs_{(particle)}$, while the contribution to toxicity of the $AgNPs_{(particle)}$ increased with increasing exposure concentrations. At the EC_{90} level, $AgNPs_{(particle)}$ dominated the toxicity. Similar findings were reported for AgNPs by Wang et al. (2012). The higher contribution to toxicity by $AgNPs_{(particle)}$ could be caused by the existence of a particle-mediated mechanism. The $AgNPs_{(particle)}$ could also enter the cell to generate reactive oxygen species, leading to damage to proteins and nucleic acids inside the bacterial cell, and finally inhibition of cell proliferation (Mcshan et al., 2014). Our study did not account for naturally relevant complexity (e.g., pH, temperature) nor compounds that can either synergistically or antagonistically affect the toxicity of AgNPs (e.g., biofilms, humic acids; Ikuma et al., 2015), but clearly hints that contributions of ions and particles in the adverse effects of NPs pollution on microbial communities largely depend on exposure levels in the environment.

The reactivity and bactericidal properties of AgNPs has been observed to change for differently sized and shaped particles (Pal et al., 2007; Sillen et al., 2015). Our results clearly showed that different shaped AgNPs severely disrupted metabolic processes of a natural soil microbial community. Studies have shown that AgNPs toxicity was size dependent at low concentrations. Ivask et al. (2014) observed that AgNPs of 1–10 nm were preferentially bound to cell membranes and were incorporated into bacteria, whereas larger AgNPs were not. In the present study, the 50 nm nanorods were found to have an EC_{50} level about two times higher than that of the 20–40 nm nanospheres and the 15 nm nanospheres. It showed that soil microbes were more vulnerable

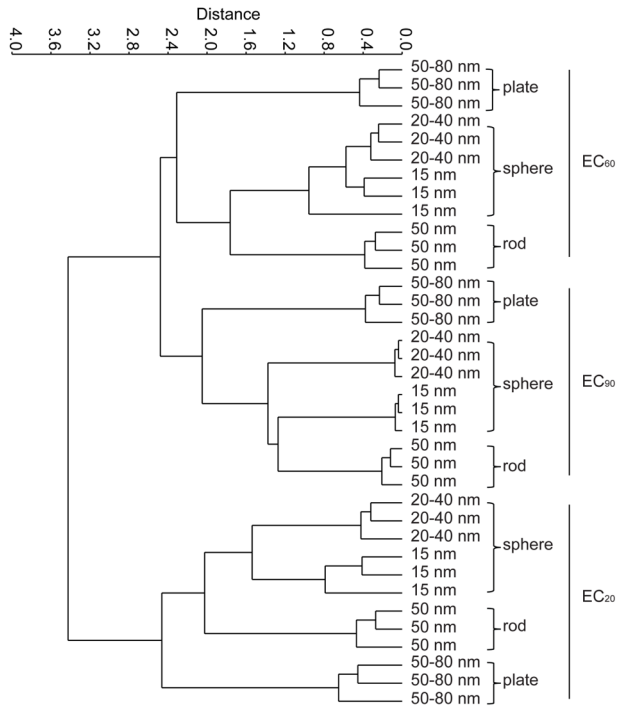

FIGURE 4 | Classifications of four different AgNPs treatments by cluster analysis according to the metabolic characteristics of the microbial communities at the EC_{20}, EC_{60}, and EC_{90} levels. Two-way ANOSIM, Euclidean-based similarity, $n = 3$, EC level $R = 0.953$, $p = 0.0001$; shape $R = 0.876$, $p = 0.0001$, respectively.

to smaller sized AgNPs than to larger sized ones. In addition, the surface area of nanosilver shapes is a key factor for controlling antimicrobial activity. The effect of AgNPs shape had also been observed in bacteria, with nanoplates showing a higher degree of toxicity (Pal et al., 2007). Sadeghi et al. (2012) also found the nanoplates solutions had a good anti-bacterial activity for both *Staphylococcus aureus* and *Escherichia coli* compared with nanorods and nanospheres. In our results, 50–80 nm nanoplates were found to be more toxic than the 50 nm nanorods. Although size was not fully represented across all our treatments and therefore prevented inference on the role of size in AgNP toxicity, these data seemed to suggest that AgNP toxicity was also size dependent. The efficient antimicrobial activity of the Ag nanoplates was ascribed to their sharp corners and edges and large areas of active crystal plane, which led to the higher amount of leaching Ag-ion (Lu et al., 2015).

Although AgNPs are well known for their anti-microbial properties, their effect on the functional diversity of natural communities remains less well understood. Our study showed that, while the overall microbial diversity and activity was comparable among treatments, the functional diversity was clearly altered depending on both concentration and shape of AgNPs. Although the use of Biolog Ecoplates did not allow firm conclusions on the actual mechanisms underlying shifts in functional diversity, it could be speculated that AgNPs alter the microbial community by adversely affecting specific enzymes and utilization of specific substrates. For instance, utilization of glycogen was inhibited in the presence of even low AgNP concentrations. Several enzymes taking part in glycogen metabolism responded to metabolites that signaled the energy need of the bacterial cell (Berg et al., 2012). Hence, the addition of AgNPs caused damage to the activation of enzymes, especially to the ones that could metabolize Glycogen. Subsequently, at higher exposure concentrations of AgNPs, the particles caused damage to the functioning of microbial communities, which likely cascaded towards distorted ecosystem processes (Kumar et al., 2011). Irrespective of the mechanism underlying our observation, AgNPs can thus clearly affect the functional composition of soil microbial communities. Disentangling naturally relevant risks, biochemical interactions and AgNPs effects on bacteria-mediated processes are thus promising areas of future research.

CONCLUSION

Our results clearly showed that the relative contribution of $AgNPs_{(particle)}$ could increase with increasing exposure concentrations and that AgNPs shape could differentially affect the functional composition of soil microbial communities. The main release routes of NPs to the environment is via wastewater effluents and deposition (McKee and Filser, 2016). As residence times of NPs in soils and sediments in general exceed typical residence times of NPs in aquatic systems, both soils and sediments can be considered the ultimate sinks of NPs in which concentrations of non-degradable or slowly degradable NPs will gradually built up. Although we used moist soil for our laboratory incubations, we thus expect that the outcome of this study also applies to aquatic sediments as AgNPs typically agglomerate in aqueous environments and thereby precipitate onto the surface of both soil and sediment particles due to the high density of Ag (e.g., Bradford et al., 2009). However, these results were obtained in simplified systems under laboratory conditions and did not include ecologically relevant compounds that potentially affect the toxicity of AgNPs. Therefore, our results should be interpreted cautiously as it remains uncertain whether patterns observed in the presently studied laboratory incubations reflected those occurring in natural systems. Not accounting for complexity likely resulted in an overestimated toxicity in our setup, yet the emerging pattern that relative contributions of ions and particles can shift depending on exposure concentrations likely resonates with relative contributions of ions and particles in natural environments. This outcome thus hints that both exposure concentrations and shape of $AgNPs_{(particle)}$ can play a significant role in the functional composition of microbial communities and in turn their associated ecosystem processes, warranting consideration of the effect of NPs on microbial functioning in environmental science and management.

AUTHOR CONTRIBUTIONS

YZ conceived the study, performed the experiments, analyzed the data and drafted the manuscript. EH helped the interpretation

of data. MW helped the Biology experiments. EH, WP and MV helped the critical revision of manuscript. All authors contributed to improve the manuscript and approved the final version of the manuscript.

FUNDING

The research described in this work was supported by the European Union Seventh Framework Programme under EC-GA No. 604602 'FUTURENANONEEDS'. MV is funded by NWO-VIDI project number 864.13.010.

ACKNOWLEDGMENT

The Chinese Scholarship Council (CSC) is gratefully acknowledged for its support to YZ (201506510003). We would like to thank Amie E. Corbin and Henrik S. Barmentlo for useful comments on our MS.

SUPPLEMENTARY MATERIAL

The Supplementary Material for this article can be found online at: http://journal.frontiersin.org/article/10.3389/fmicb.2016.01123

REFERENCES

Berg, J. M., Tymoczko, J. L., and Stryer, L. (2012). *Biochemistry*. 7th Edn. New York, NY: W. H. Freeman, 338.

Bradford, A., Handy, R. D., Readman, J. W., Atfield, A., and Mühling, M. (2009). Impact of silver nanoparticle contamination on the genetic diversity of natural bacterial assemblages in estuarine sediments. *Environ. Sci. Technol.* 43, 4530–4536. doi: 10.1021/es9001949

Dinesh, R., Anandaraj, M., Srinivasan, V., and Hamza, S. (2012). Engineered nanoparticles in the soil and their potential implications to microbial activity. *Geoderma* 173–174, 19–27. doi: 10.1016/j.geoderma.2011.12.018

Echavarri-Bravo, V., Paterson, L., Aspray, T. J., Porter, J. S., Winson, M. K., Thornton, B., et al. (2015). Shifts in the metabolic function of a benthic estuarine microbial community following a single pulse exposure to silver nanoparticles. *Environ. Pollut.* 201, 91–99. doi: 10.1016/j.envpol.2015.02.033

Garland, J. L. (1999). "Potential and limitations of BIOLOG for microbial community analysis," in *Proceedings of the 8th International Symposium on Microbial Ecology, Microbial Biosystems: New Frontiers*, eds C. R. Bell, M. Brylinski, and P. Johnson-Green (Hailfax: Atlantic Canada Society for Microbial Ecology), 1–7.

Garland, J. L., and Mills, A. L. (1991). Classification and characterization of heterotrophic microbial communities on the basis of patterns of community-level sole-carbon-source utilization. *Appl. Environ. Microbiol.* 57, 2351–2359.

Ge, Y., Schimel, J. P., and Holden, P. A. (2011). Evidence for negative effects of TiO2 and ZnO nanoparticles on soil bacterial communities. *Environ. Sci. Technol.* 45, 1659–1664. doi: 10.1021/es103040t

George, S., Lin, S., Ji, Z., Thomas, C. R., Li, L., Mecklenburg, M., et al. (2012). Surface defects on plate-shaped silver nanoparticles contribute to its hazard potential in a fish gill cell line and zebrafish embryos. *ACS Nano* 6, 3745–3759. doi: 10.1021/nn204671v

González, A. G., Mombo, S., Leflaive, J., Lamy, A., Pokrovsky, O. S., and Rols, J. L. (2015). Silver nanoparticles impact phototrophic biofilm communities to a considerably higher degree than ionic silver. *Environ. Sci. Pollut. Res. Int.* 22, 8412–8424. doi: 10.1007/s11356-014-3978-1

Gorka, D. E., Osterberg, J. S., Gwin, C. A., Colman, B. P., Meyer, J. N., Bernhardt, E. S., et al. (2015). Reducing environmental toxicity of silver nanoparticles through shape control. *Environ. Sci. Technol.* 49, 10093–10098. doi: 10.1021/acs.est.5b01711

Hammer, Ø., Harper, D. A. T., and Ryan, P. D. (2001). PAST: paleontological statistics software package for education and data analysis. *Palaeontol. Electron.* 4:9.

Hänsch, M., and Emmerling, C. (2010). Effects of silver nanoparticles on the microbiota and enzyme activity in soil. *J. Plant Nutrit. Soil Sci.* 173, 554–558. doi: 10.1002/jpln.200900358

Hua, J., Vijver, M. G., Richardson, M. K., Ahmad, F., and Peijnenburg, W. J. (2014). Particle-specific toxic effects of differently shaped zinc oxide nanoparticles to zebrafish embryos (*Danio rerio*). *Environ. Toxicol. Chem.* 33, 2859–2868. doi: 10.1002/etc.2758

Hund-Rinke, K., and Schlich, K. (2014). The potential benefits and limitations of different test procedures to determine the effects of Ag nanomaterials and $AgNO_3$ on microbial nitrogen transformation in soil. *Environ. Sci. Eur.* 26:28. doi: 10.1186/s12302-014-0028-z

Hunting, E. R., Mulder, C., Kraak, M. H. S., Breure, A. M., and Admiraal, W. (2013a). Effects of copper on invertebrate-sediment interactions. *Environ. Pollut.* 180, 131–135. doi: 10.1016/j.envpol.2013.05.027

Hunting, E. R., Vijver, M. G., Van der Geest, H. G., Mulder, C., Kraak, M. H. S., Breure, A. M., et al. (2015). Resource niche overlap promotes stability of bacterial community metabolism in experimental microcosms. *Front. Microbiol.* 6:105. doi: 10.3389/fmicb.2015.00105

Hunting, E. R., White, C. M., Van Gemert, M., Mes, D., Stam, E., Van der Geest, H. G., et al. (2013b). UV radiation and organic matter composition shape bacterial functional diversity in sediments. *Front. Microbiol.* 4:317. doi: 10.3389/fmicb.2013.00317

Ikuma, K., Decho, A. W., and Lau, B. L. (2015). When nanoparticles meet biofilms-interactions guiding the environmental fate and accumulation of nanoparticles. *Front. Microbiol.* 6:591. doi: 10.3389/fmicb.2015.00591

Ivask, A., Kurvet, I., Kasemets, K., Blinova, I., Aruoja, V., Suppi, S., et al. (2014). Size-dependent toxicity of silver nanoparticles to bacteria, yeast, algae, crustaceans and mammalian cells in vitro. *PLoS ONE* 9:e102108. doi: 10.1371/journal.pone.0102108

Kendra, L. G., and Arturo, A. K. (2014). Emerging patterns for engineered nanomaterials in the environment: a review of fate and toxicity studies. *J. Nanopart. Res.* 16, 2503–2530. doi: 10.1007/s11051-014-2503-2

Kermanizadeh, A., Gaiser, B. K., Hutchison, G. H., and Stone, V. (2012). An in vitro liver model-assessing oxidative stress and genotoxicity following exposure of hepatocytes to a panel of engineered nanomaterials. *Part. Fibre Toxicol.* 9:28. doi: 10.1186/1743-8977-9-28

Krause, S., Le Roux, X., Niklaus, P. A., Van Bodegom, P. M., Lennon, J. T., Bertilsson, S., et al. (2014). Trait-based approaches for understanding microbial biodiversity and ecosystem functioning. *Front. Microbiol.* 5:251. doi: 10.3389/fmicb.2014.00251

Kumar, N., Shah, V., and Walker, V. K. (2011). Perturbation of an arctic soil microbial community by metal nanoparticles. *J. Hazard. Mater.* 190, 816–822. doi: 10.1016/j.jhazmat.2011.04.005

Lau, J. A., and Lennon, J. T. (2012). Rapid responses of soil microorganisms improve plant fitness in novel environments. *Proc. Natl. Acad. Sci. U.S.A.* 109, 14058–14062. doi: 10.1073/pnas.1202319109

Levard, C., Hotze, E. M., Lowry, G. V., and Brown, G. E. Jr. (2012). Environmental transformations of silver nanoparticles: impact on stability and toxicity. *Environ. Sci. Technol.* 46, 6900–6914. doi: 10.1021/es2037405

Levard, C., Mitra, S., Yang, T., Jew, A. D., Badireddy, A. R., Lowry, G. V., et al. (2013). Effect of chloride on the dissolution rate of silver nanoparticles and toxicity to *E. coli*. *Environ. Sci. Technol.* 47, 5738–5745. doi: 10.1021/es400396f

Lu, W., Yao, K., Wang, J., and Yuan, J. (2015). Ionic liquids-water interfacial preparation of triangular Ag nanoplatess and their shape-dependent antibacterial activity. *J. Colloid Interface Sci.* 437, 35–41. doi: 10.1016/j.jcis.2014.09.001

McKee, M. S., and Filser, J. (2016). Impacts of metal-based engineered nanomaterials on soil communities. *Environ. Sci. Nano* 3, 506–533. doi: 10.1039/c6en00007j

McQuillan, J. S., Infante, H. G., Stokes, E., and Shaw, A. M. (2011). Silver nanoparticle enhanced silver ion stress response in *Escherichia coli* K12. *Nanotoxicology* 6, 857–866. doi: 10.3109/17435390.2011.626532

Mcshan, D., Ray, P. C., and Yu, H. (2014). Molecular toxicity mechanism of nanosilver. *J. Food Drug Anal.* 22, 116–127. doi: 10.1016/j.jfda.2014.01.010

Pal, S., Tak, Y. K., and Song, J. M. (2007). Does the antibacterial activity of silver nanoparticles depend on the shape of the nanoparticle? A study of the gram-negative bacterium *Escherichia coli*. *Appl. Environ. Microbiol.* 73, 1712–1720. doi: 10.1128/AEM.02218-06

Sadeghi, B., Garmaroudi, F. S., Hashemi, M., Nezhad, H. R., Nasrollahi, A., Ardalan, S., et al. (2012). Comparison of the anti-bacterial activity on the nanosilver shapes: nanoparticles, nanorodss and nanoplatess. *Adv. Powder Technol.* 23, 22–26. doi: 10.1016/j.apt.2010.11.011

Schlich, K., Klawonn, T., Terytze, K., and Hund-Rinke, K. (2013). Hazard assessment of a silver nanoparticle in soil applied via sewage sludge. *Environ. Sci. Eur.* 25:17. doi: 10.1186/2190-4715-25-17

Shannon, C. E. (1948). A mathematical theory of communication. *Bell Syst. Tech. J.* 27, 379–423. doi: 10.1145/584091.584093

Sillen, W. M. A., Thijs, S., Abbamondi, G. R., Janssen, J., Weyens, N., White, J. C., et al. (2015). Effects of silver nanoparticles on soil microorganisms and maize biomass are linked in the rhizosphere. *Soil Biol. Biochem.* 91, 14–22. doi: 10.1016/j.soilbio.2015.08.019

Theophel, K., Schacht, V. J., Schlüter, M., Schnell, S., Stingu, C. S., Schaumann, R., et al. (2014). The importance of growth kinetic analysis in determining bacterial susceptibility against antibiotics and silver nanoparticles. *Front. Microbiol.* 5:544. doi: 10.3389/fmicb.2014.00544

Tlili, A., Cornut, J., Behra, R., Gil-Allué, C., and Gessner, M. O. (2016). Harmful effects of silver nanoparticles on a complex detrital model system. *Nanotoxicology* 10, 728–735. doi: 10.3109/17435390.2015.1117673

Topuz, E., and van Gestel, C. A. (2015). Toxicokinetics and toxicodynamics of differently coated silver nanoparticles and silver nitrate in enchytraeus crypticus upon aqueous exposure in an inert sand medium. *Environ. Toxicol. Chem.* 34, 2816–2823. doi: 10.1002/etc.3123.

Van der Ploeg, M. J. C., Handy, R. D., Waalewijn-Kool, P. L., van den Berg, J. H. J., Herrera Rivera, Z. E., Bovenschen, J., et al. (2014). Effects of silver nanoparticles (NM-300K) on *Lumbricus rubellus* earthworms and particle characterization in relevant test matrices including soil. *Environ. Toxicol. Chem.* 33, 743–752. doi: 10.1002/etc.2487

Villéger, S., Mason, N. W. H., and Mouillot, D. (2008). New multidimensional functional diversity indices for a multifaceted framework in functional ecology. *Ecology* 89, 2290–2301. doi: 10.1890/07-1206.1

Wang, Z., Chen, J., Li, X., Shao, J., and Peijnenburg, W. J. (2012). Aquatic toxicity of nanosilver colloids to different trophic organisms: contributions of particles and free silver ion. *Environ. Toxicol. Chem.* 31, 2408–2413. doi: 10.1002/etc.1964

Wang, Z.-G., Hu, Y.-L., Xu, W.-H., Liu, S., Hu, Y., and Zhang, Y. (2015). Impacts of dimethyl phthalate on the bacterial community and functions in black soils. *Front. Microbiol.* 6:405. doi: 10.3389/fmicb.2015.00405

Weber, K. P., Grove, J. A., Gehder, M., Anderson, W. A., and Legge, R. L. (2007). Data transformations in the analysis of community-level substrate utilization data from microplates. *J. Microbiol. Methods* 69, 461–469. doi: 10.1016/j.mimet.2007.02.013

Yang, X., Jiang, C., Hsu-Kim, H., Badireddy, A. R., Dykstra, M., Wiesner, M., et al. (2014). Silver nanoparticle behavior, uptake, and toxicity in *Caenorhabditis elegans*: effects of natural organic matter. *Environ. Sci. Technol.* 48, 3486–3495. doi: 10.1021/es404444n

Yu, S., Yin, Y., and Liu, J. (2013). Silver nanoparticles in the environment. *Environ. Sci. Process. Impacts* 15, 78–92. doi: 10.1039/C2EM30595J

Zhao, C. M., and Wang, W. X. (2012). Importance of surface coatings and soluble silver in silver nanoparticles toxicity to *Daphnia magna*. *Nanotoxicology* 6, 361–370. doi: 10.3109/17435390.2011.579632

Conflict of Interest Statement: The authors declare that the research was conducted in the absence of any commercial or financial relationships that could be construed as a potential conflict of interest.